2 Houlberg W A, Attenberger S E, Bayler L R, et al. Pellet Penetration Experiment on JET. Nucl. Fusion, 1992, 32(11): 1951
3 Baylor L R, Schmidt G L, Batha S H, et al. Pellet Fuelled Enhanced Confinement ICRF Discharges in TFTR. Nucl. Fusion, 1997, 37 (1): 127
4 Pecquet A L, Cristofani P, Mattioli M, et al. Snake-like Phenomena in Tore Supra Following Pellet Injection. Nucl. Fusion, 1997, 37 (4): 451
5 Liu W, Talvard M. Rapid Global Response of the Electron Temperature during Pellet Injection on Tore Supra. Nucl. Fusion, 1994, 34(3): 337
6 Lang P T, Buckl K, Kaufmann, et al. High-efficiency Plasma Refuelling by Pellet Injection from the Magnetic High-field Side into ASDEX-up. Phys. Rev. Lett., 1997, 79: 1487
7 Baylor L R, Jernigan T C, Houlberg W A, et al. Improved Core Fueling with High Field Side Pellet Injection in the DⅢ-D Tokamak. Phys. Plasma, 2000, 7(5): 1878
8 Durst R D, Phillips P E, Rowan W L. Q-profile Measurement in Tokamaks Using Fuelling Pellets. Rev. Sci. Intru., 1988, 59(8): 1623
9 XIAO Zhenggui, LI Bo, LI Li, et al. Plasma Performance with Multi-shot Pellet Fueling in the HL-1M Tokamak. Nuclear Fusion and Plasma Fusion (in Chinese), 1999, 19(3): 164
10 DONG Jiafu, LUO Junlin, TANG Nianyi, et al. Analysis of Pellet Penetration and Confinement Characteristic in the HL-1M Tokamak. Nuclear Fusion and Plasma Physics (in Chinese), 2000, 20(2): 103
11 ZHENG Yinjia, FENG Zhen, LIU Yong, et al. Pellet cloud Analysis and Preliminary *q*-Profile Measurement on the HL-1M Tokamak. Nuclear Fusion and Plasma Fusion (in Chinese), 2000, 20(4): 232
12 Parks P B, Turbull R J, Foster C A. A Model for the Ablation Rate of a solid Hydrogen pellet in a plasma. Nucl. Fusion, 1997, 17(3): 539
13 Kuteev B V. Hydrogen Pellet Ablation and Acceleration by Current in High Temperature Plasma. Nucl. Fusion, 35, 1995(4): 431

1.7 Ablation Characteristics and Sawtooth Phenomena in the HL-1M Pellet Fuelling Plasma

XIAO Zhenggui DONG Jiafu GUO Gancheng ZHENG Yinjia
LI Bo LI Li LIU Yong WANG Enyao

Key word Pellet fuelling Ablation Sawtooth

In recent years pellet injection (PI) experiments have been performed at HL-1M to study the characteristics of plasma with peaking density profile and to improve confinement. The works are focused on the relation of MHD activity and improved confinement on the pellet penetration depth and the process of pellet ablation in the plasma.

In HL-1M PI, the H_α and soft X-ray signals are obtained with two sets of PIN diode arrays. The pellet cloud image with ten exposures and the images of multi-pellet ablated in one discharge as well as some useful information on pellet ablation have been obtained with a CCD camera. According to the variance of the inclination angle of the pellet ablation cloud in different radii(r), the $q(r)$ of the HL-1M plasma is estimated.

1 Experimental set-up and diagnostics

The experimental set-up and main diagnostics are shown in Fig. 1.

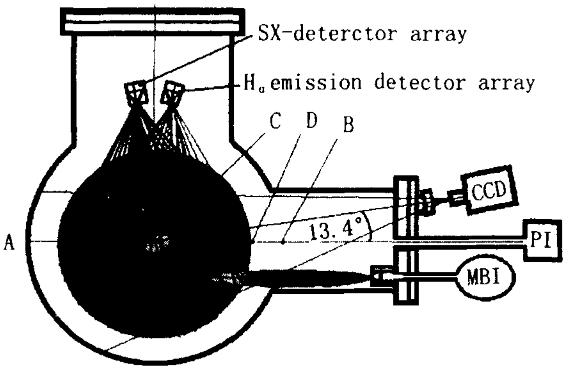

Fig. 1 Experimental set-up

In HL-1M the H_α detectors and a soft X-ray (SX) detectors with 20 channels of PIN diode respectively are located on the top of the same poloidal cross section of pellet injection port. The sight line of two detectors is vertically covered the full poloidal section.

The SensiCam 360LF CCD camera is mounted 8.7 cm above and formed an angle of 13.4° with respect to the pellet injection line. The line sight of camera can cover the horizontal pellet path in plasma.

2 Experimental results

2.1 Sawtooth phenomena and MHD activity

The sawteeth appeared in nearly all kind of tokamak discharges, some models assume they are MHD instability and can be influenced by PI. The variances of MHD activity have been observed in HL-1M with PI discharges. In most of HL-1M PI discharges, the instabilities are suppressed especially in deep pellet injection, sometimes, the instabilities are excited by pellet.

When the pellets penetrate into center region the sawtooth and the precursor oscillation of $m = 1$ mode were be suppressed, the $q = 1$ surface disappear and the current profile of plasma is flattened as shown in Fig. 2.

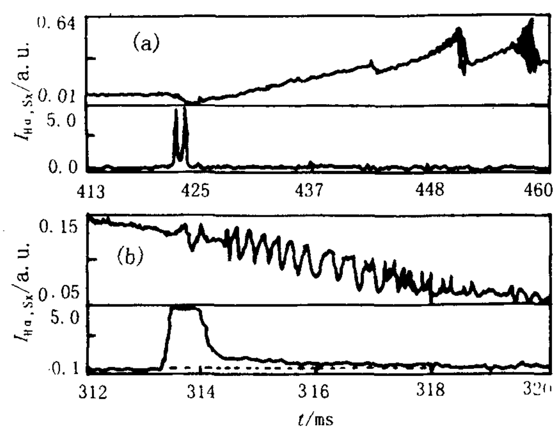

Fig. 2 (a) The sawtooth and precursor oscillation of $m = 1$ mode and (b) the saturation $m = 1$ mode are suppressed, $q = 1$ surface is disappear by pellet

The sawtooth activity were suppressed for 30 ~ 50 ms as pellets penetrating into or close to $q = 1$ surface. In some cases the sawtooth is suppressed by pellet but $m = 1$ mode still present, it means the plasma current profile is still peaked, only the internal disruption are suppressed.

When T_e and N_e are lower before PI, the T_e dropped rapidly and the N_e profile became very peaked in short time (10 ms) after PI. The intensity of SX emission in center region rises and an $m = 1$ mode superimposed on it, the $q = 1$ surface appears, it may be due to the sharp increase of N_e gradient that leads the discharge into sawtooth oscillation region in Fig. 3(a). In Fig. 3(b), a large $m = 1$ mode is immediately excited but the internal disruption of sawtooth oscillation were not observed, the turbulence of $m = 1$ mode superimposed on signals of T_e and N_e. In this case the profile of T_e keeps peaking and the amplitude of T_e does not drop, the plasma current channel became narrow, this implies that the pellet only deposited at the outer region of plasma.

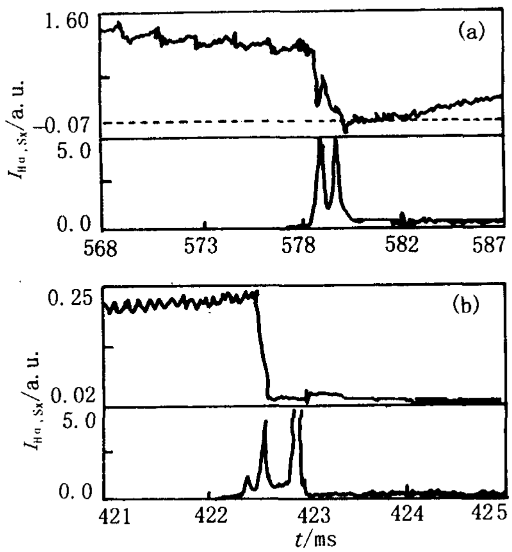

Fig. 3 (a) The intensity of SX emission risen in center region of plasma, the $q = 1$ surface appears by pellet, (b) the $m = 1$ mode with large amplitude excited by large pellet

2.2 Observation of pellet penetration

The temporal and spatial evolution of H_α emission is usually used to analyze the deposition and penetration depth λ_p of pellet in plasma.

When pellet enter into the hot plasma, a cloud ($10^{23} \sim 10^{24}$ m^{-3}) with high dense and cold (several eV) plasmoid forms and moved with the pellet. These plasmoid contain a fraction of neutral atoms and non-fully ionized ions and emitted visible light of H_α, which is directly proportional to the pellet ablation rate. We think that the position of the peaking value H_α indicates the position of the pellet in plasma. In HL-1M PI discharges the λ_p has been measured by means of multi-channel H_α emission signal and Abel inversion method. The λ_p is in the range of 110 ~ 260 mm.

The average velocity v_a of ablation cloud moved in the plasma is estimated by $\Delta\lambda_p/\Delta t$. The ablation cloud traveled over 11 cm in 0.29 ms, so the v_a is ~400 $m \cdot s^{-1}$. However, the free flying velocity v_f of the pellet before it entering plasma is 460 $m \cdot s^{-1}$ in this shot. We noted that the v_p is slower than v_f and the deeper the pellet penetration the slower the v_p, as shown in Fig. 4.

In the HL-1M experiments the deposition region of fuelling particles for gas puffing (GP) and molecular beam injection (MBI) were measured also by same H_α detector array. In MBI, the particle deposited mainly at the outer region in the half of the plasma. The peaked profile of N_e also could be obtained usually in the later period (~300 ms) of the MBI. It seems that the drift of ionized particles plays an important role in this phenomenon. The fueling efficiency and confinement performances of PI are always better than MBI and GP in the medium average N_e. It indicated that the center region deposition of fueling particles plays an important role in the improved confinement.

2.3 Photograph of pellet ablation process

In PI discharges, some typical image pho-

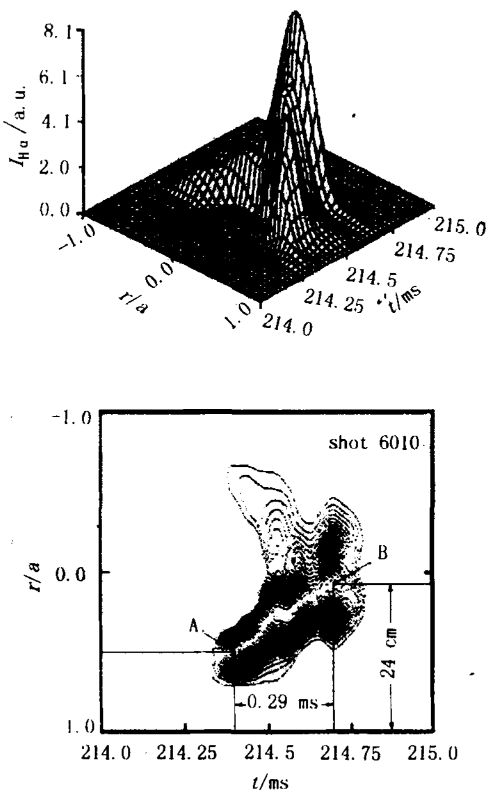

Fig. 4 Typical temporal and spatial evolution of H_α line emission intensity for pellet injection (up) and the its contour plot(low)

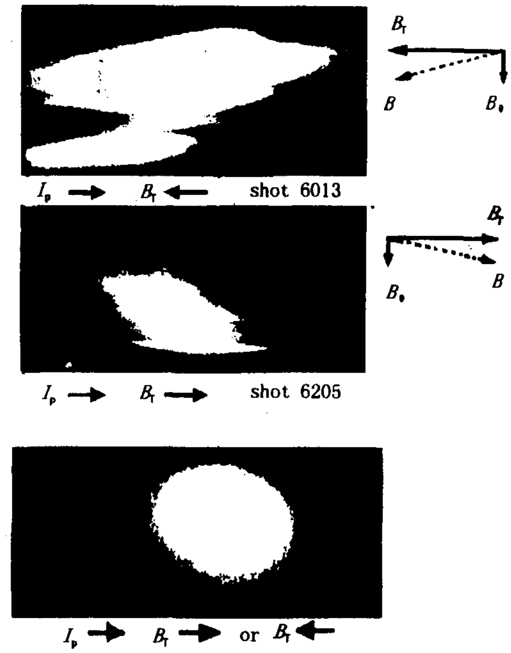

Fig. 5 The typical photos and a reversal direction of the inclination angle of the pellet cloud is observed with the toroidal magnetic field inverted (up), but the photos of MBI keeps same shape (low)

tos of ablation cloud have been obtained with CCD camera as shown in Fig. 5.

Usually, when the pellet injected into $q=2$ surface, the elongation of pellet ablation cloud along the local magnetic field direction (thus forming an in situ field line map) and the inclination angle of cloud with respect to the toroidal direction are clear. When toroidal B_T inversed the inclination angle of clouds reversed too, it means that the photos respond truly the ablation process of the pellet. However, the pattern of the photos with MBI always keeps same even though the toroidal field direction inverted Fig. 5(low). Although the ablation mechanism and the photo shape of MBI are not completely understood now, comparison the Fig. 5 (low) and photo obtained with medium pellet injection previously, the deposition region of MBI is consistent with its photo shape in the plasma.

3 Summary

In the HL-1M experiments, PI influences the MHD activity and the confinement of plasma. In most of PI discharges, the central MHD instabilities are suppressed, the peaked density profile and improved confinement are obtained, especially in deep pellet injection. Sometime, in the discharges with lower N_e and T_e the instabilities are excited by pellet.

The analyses of temporal and spatial evolution of H_α emission for PI, MBI, GP indicated that the deposit region of particles plays an important role for improving confinement of plasma. The motion velocity of pellet ablation cloud v_p is always slower than v_f, the deeper the pellet injection the slower the v_p.

The elongation along the magnetic field the variance of inclination angle α' of the pellet ablation cloud at different minor radii of plasma are observed by an ablation cloud photo with ten-exposure CCD camera. According to this observation the q-profile of the HL-1M plasma in center region is estimated.

1.8 Edge Structure of Reynolds Stress and Poloidal Flow in the HL-1M Tokamak

HONG Wenyu WANG Enyao CAO Jianyong LI Qiang LIU Dazhi

Key words Reynolds stree Poloidal flow velocity Radial and poloidal electric field

The determination of electrostatic Reynolds stress and plasma poloidal flow velocity in scrape-off layer (SOL) and the boundary of tokamak plasma have become of prime importance due to its possible role in confinement and the L-H mode transition [1,2]. The plasma confinement is sensitive to the edge conditions. Theoretically, various mechanisms have been proposed to explain the creation of sheared poloidal flow. In brief, theories attempt to explain the L-H transition focus on the turbulence-induced Reynolds stress, colloidal velocity v_c and radial electric field E_r structure at the edge. Turbulence Reynolds stress plays a linking role between the turbulence and averaged flows.

Measurements were carried out in the LHCD, SMBI, MBI and NBI experiments of the HL-1M tokamak. In recent experiments, plasma performance was greatly improved through the use of boronization, siliconization, and lithiumization. Typical parameters of ohmic heated hydrogen plasma are: $n_e<8\times10^{19}$ m^{-3}, $I_p<320$ kA, $B_T<3$ T, electron temperature $T_e(0)=0.5\sim1$ keV and ion temperature $T_i(0)=0.3\sim0.8$ keV, a pulse duration of up to 4 s. LHCD at a power level of 1 MW, NBI at a power level of 0.4 MW have been initiated. New fueling technique with pellet injection and supersonic SMBI and MPI were also employed to significantly improve the energy confinement time and density limit.

Neglecting the contribution of magnetic fluctuations, the Reynolds stress Re was determined by $Re=\langle\tilde{v}_r\tilde{v}_\theta\rangle$. The $\langle\tilde{v}_r\tilde{v}_\theta\rangle$ term of the Reynolds stress tensor can be related to the $\boldsymbol{E}\times\boldsymbol{B}$ drift velocities, it can be determined using the expression [1,2]:

$$\langle\tilde{v}_r\tilde{v}_\theta\rangle=-\langle\tilde{E}_r\tilde{E}_\theta\rangle/B^2 \qquad (1)$$

where $\tilde{v}_r$ and $\tilde{v}_\theta$ is the fluctuating radial and poloidal flow velocities of edge plasma re-